

## Quantum phase transition between one-channel and two-channel Kondo polarons

Julián Rincón,<sup>1</sup> Daniel J. García,<sup>2</sup> K. Hallberg,<sup>2</sup> and Matthias Vojta<sup>3</sup>

<sup>1</sup>Center for Nanophase Materials Sciences, Oak Ridge National Laboratory, Oak Ridge, Tennessee 37831, USA

<sup>2</sup>Instituto Balseiro, Centro Atómico Bariloche, CNEA and CONICET, 8400 Bariloche, Argentina

<sup>3</sup>Institut für Theoretische Physik, Technische Universität Dresden, 01062 Dresden, Germany

(Received 3 July 2013; published 31 October 2013)

For a mobile spin-1/2 impurity, coupled antiferromagnetically to a one-dimensional gas of fermions, perturbative ideas have been used to argue in favor of two-channel Kondo behavior of the impurity spin. Here we combine general considerations and extensive numerical simulations to show that the problem displays a novel quantum phase transition between two-channel and one-channel Kondo screening upon increasing the Kondo coupling. We construct a ground-state phase diagram and discuss the various nontrivial crossovers as well as possible experimental realizations.

DOI: [10.1103/PhysRevB.88.140407](https://doi.org/10.1103/PhysRevB.88.140407)

PACS number(s): 67.85.Lm, 05.30.Rt, 67.30.hm, 72.15.Qm

The problem of dilute particles moving in quantum liquids finds realizations in diverse areas of modern physics,<sup>1</sup> such as charge carriers in weakly doped semiconductors or Mott insulators, ions in <sup>3</sup>He, muons in metals, electrons in multiband quantum wires, and multicomponent ultracold gases with a strong population imbalance.<sup>2</sup> For dilute particles with internal degrees of freedom, e.g., spin, a connection to quantum impurity problems, such as the Kondo effect, is natural. Indeed, a recent paper<sup>3</sup> argued that a spinful particle moving in a one-dimensional (1D) electron gas creates a Kondo polaron which realizes the two-channel Kondo (2CK) effect. This remarkable many-body effect occurs if a spin 1/2 is *overscreened* by the coupling to two equivalent screening channels of conduction electrons, leading to exotic non-Fermi-liquid behavior.<sup>4–6</sup> (For the 2CK polaron of Ref. 3 the two screening channels are realized by independent left- and right-moving bath fermions.) While an unambiguous verification of 2CK behavior in solids containing magnetic ions is still a challenge,<sup>7</sup> success was reported<sup>8</sup> for a nanostructured device consisting of a quantum dot with two reservoirs.

The 2CK effect is unstable with regard to channel asymmetry, such that the 2CK fixed point can be understood as a critical point separating two single-channel Kondo (1CK) phases. However, settings with a true quantum phase transition (QPT)<sup>9,10</sup> between 1CK and 2CK phases are rare: The only example known to us is a proposal involving a quantum dot coupled to helical edge states of a topological insulator.<sup>11</sup> In contrast, for an impurity coupled to a standard Luttinger liquid, it has been argued that either a 1CK or a 2CK phase is stable depending on the host's Luttinger parameter,<sup>12</sup> but a QPT upon varying an impurity parameter does not occur.

In this Rapid Communication, we shall argue that the Kondo-polaron model of Ref. 3 realizes a novel QPT between 1CK and 2CK polarons. We consider a single spin-1/2 particle, henceforth called “impurity”, which moves in a 1D gas of spin-1/2 fermions. The two species (or bands) are coupled by an antiferromagnetic exchange interaction  $J$ . The full lattice Hamiltonian reads

$$\mathcal{H} = - \sum_{(ij)\sigma} (tc_{i\sigma}^\dagger c_{j\sigma} + t'd_{i\sigma}^\dagger d_{j\sigma}) + \sum_{i=1}^L (J\vec{S}_i \cdot \vec{s}_i + hS_i^z), \quad (1)$$

where  $n_i = \sum_{\sigma} c_{i\sigma}^\dagger c_{i\sigma}$  and  $\vec{s}_i = \sum_{\sigma\sigma'} c_{i\sigma}^\dagger \vec{\tau}_{\sigma\sigma'} c_{i\sigma'}$ , with  $\vec{\tau}$  the Pauli matrices, denote the local charge and spin densities, respectively, of the bath fermions. Their total density is  $n_c = \sum_i n_i/L$  and their bandwidth  $W = 4t$ . The impurity is described by  $d$  operators, with local densities  $N_i$  and  $\vec{S}_i$  and a total filling of one particle,  $\sum_i N_i = 1$ . A magnetic field  $h$  coupling to the impurity is included.

The purpose of this Rapid Communication is a discussion of the full parameter space of the model (1), beyond the weak-coupling limit considered in Ref. 3. To this end, we combine the analysis of various strong-coupling limits with comprehensive numerical studies. Our central result is that a QPT generically separates a small- $J$  phase with 2CK screening of the impurity spin<sup>3</sup> from a 1CK phase at stronger coupling  $J$ , as summarized in the phase diagram in Fig. 1. The transition in Eq. (1) thus involves a change from local non-Fermi-liquid to Fermi-liquid behavior upon increasing  $J$ , accompanied by a jump in the residual impurity entropy from  $\ln \sqrt{2}$  to 0.<sup>6</sup> The transition is driven by varying only impurity parameters,  $J$  or  $t'$ , while keeping the bath parameters fixed, and corresponds to a hitherto unknown QPT.

In addition to the 1CK-2CK transition, we uncover an interesting strong-coupling regime, where the motion of the impurity locally suppresses charge fluctuations in the electron gas, thereby generating a “correlation cloud” (or “correlation polaron”) whose size,  $\xi_c$ , is dictated by kinetic energy and can be much larger than that of the Kondo screening cloud,  $\xi_K$ .

In the body of this Rapid Communication, we present general arguments and numerical results from the density matrix renormalization group (DMRG) which lead to the above conclusions. In the impurity's magnetic response, we find universal behavior in each phase which we use to characterize them. We also discuss possible realizations of the phenomena in the field of ultracold atomic gases; we note that related impurity problems have been recently studied using cold bosonic atoms in optical lattices.<sup>13</sup>

*Weak-coupling limit*,  $T_K^0 \ll t' \ll t$ . We begin by summarizing the physics of the model (1) in the limit of small  $J$ , discussed in Ref. 3. We use  $T_K^0$  as shorthand for the Kondo temperature of a static impurity coupled with exchange  $J$  to a band of width  $W$ ; for  $J \ll t$  we have  $\ln(T_K^0/W) \propto -W/J$ . The fate of the magnetic moment can be accessed in an expansion

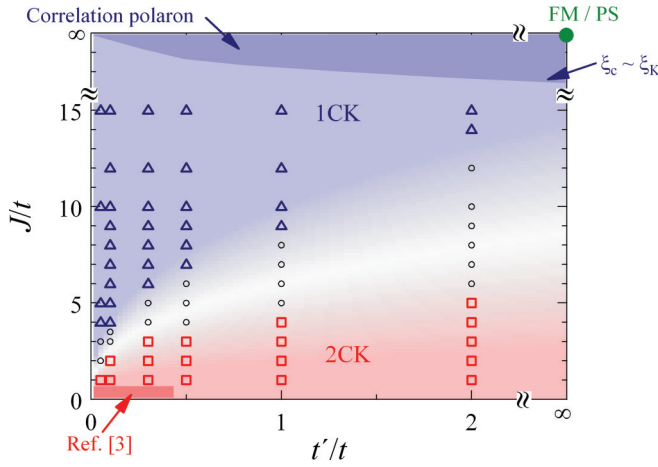


FIG. 1. (Color online) Ground-state phase diagram of the Kondo-polaron model, Eq. (1), obtained from DMRG at  $n_c = 1$ . Triangles (squares) denote parameters with 1CK (2CK) behavior. The two phases are separated by a QPT in the thermodynamic limit; in our finite-size numerics this transition is smeared, with circles corresponding to parameters in the crossover region. At large  $J$ , a correlation polaron forms, with size  $\xi_c \ll \xi_K$ . For  $t = 0$  and finite  $t'/J$ , kinetic ferromagnetism (FM) is realized at  $n_c = 1$ , while phase separation (PS) occurs away from half filling (schematically shown).

in  $J$  around the decoupled  $J = 0$  fixed point. This expansion is similar to the standard weak-coupling expansion in the Kondo model, with the key difference being that the recoil energy of the impurity renders  $2k_F$  backscattering processes from  $J$  to be absent from the low-energy sector. Hence, only processes with small momentum transfer—involving either left movers near  $(-k_F)$  or right movers near  $k_F$ —contribute to the logarithmic singularities, leading to flow equations equivalent to that of the 2CK effect. In other words, the motion of the Kondo impurity causes left-moving and right-moving  $c$  fermions to form two separate screening channels for the impurity spin.

Importantly, this argument in favor of 2CK physics requires both  $T_K^0 \ll t'$ , as otherwise the recoil is too small to be relevant, and  $T_K^0 \ll t$ , as otherwise the separation into left movers and right movers is not justified.

*Strong-coupling limit,  $J \gg t \gg t'$ .* In the limit  $J \rightarrow \infty$  the impurity electron locks into a singlet with one conduction electron. For  $t' = 0$  this singlet is immobile and effectively cuts the 1D electron gas. From first-order perturbation theory in  $t'$  one finds that the singlet forms a Bloch wave with a kinetic energy of order  $t'$ . Clearly, this corresponds to a slowly moving 1CK polaron of minimal size, i.e., 1CK physics is realized in this limit.

*Strong-coupling limit,  $J \gg t' \gtrsim t$ .* It is interesting to discuss the evolution of the singlet polaron upon increasing  $t'/t$ . Whereas for  $t'/t \rightarrow 0$  the conduction electrons simply adjust to the position of the singlet, the case  $t' \gtrsim t$  implies a faster motion of the polaron which is only possible (without breaking the singlet) along a sequence of singly occupied  $c$  sites. As a result, the  $c$ -electron kinetic energy will be quenched in a vicinity of size  $\xi_c$  of the impurity. Within this *correlation polaron* the impurity moves with a kinetic energy of order  $t'$ , while the polaron itself—consisting of the singlet surrounded by singly occupied  $c$  sites—is a heavy object with kinetic

energy of order  $t$  (in a manner similar to the ferromagnetic Kondo polaron described in Ref. 14). A variational estimate, assuming an immobile correlation polaron, yields  $\xi_c \propto t'/t$ . Thus, the correlation polaron emerges from the competition of impurity and  $c$ -electron kinetic energies in the large- $J$  limit.

*Nagaoka limit,  $t = 0$ .* For completeness, we also mention the case of immobile  $c$  electrons,  $t = 0$ . Consistent with the above discussion,  $\xi_c \rightarrow \infty$  in this limit, i.e., the motion of the impurity electron, prefers singly occupied  $c$  sites in the entire system. While the spin alignment on the  $c$  sites can be arbitrary for  $J = \infty$ , ferromagnetic alignment is preferred for any finite  $t'/J$ —this kinetic magnetism can be understood as double-exchange or Nagaoka ferromagnetism. If  $n_c$  deviates from half filling, the system consequently phase separates into a half-filled ferromagnetic region and a region where  $\langle n_i \rangle \neq 1$ .

For both  $t$  and  $t'$  finite and small compared to  $J$ , the tendency towards ferromagnetic alignment survives *inside* the correlation polaron. A detailed study of this interesting regime is beyond the scope of this Rapid Communication.

*Expected QPT.* As argued above, 2CK screening is realized for  $T_K \ll \min(t', t)$ , where  $T_K$  is now a Kondo temperature in the presence of  $t'$ . On the other hand, the 1CK state of an immobile impurity ( $t' = 0$ ) can be expected to be stable against small  $t' \ll T_K$  (the 1CK polaron simply starts to move). Hence, a transition from 2CK to 1CK will occur upon increasing  $J$  or decreasing  $t'$ , as indeed confirmed by our numerics (Fig. 1).

*DMRG results.* We have studied the model (1) using the DMRG technique<sup>15,16</sup> on finite systems with  $2 \times L$  lattice sites. As the open boundary conditions commonly used with DMRG lead to boundary pinning of the impurity electron, we have instead used antiperiodic boundary conditions (APBCs), with  $L < 40$ . This implies that Kondo screening with small  $T_K < 10^{-2}t$  will be hard to observe due to  $\xi_K \gg L$ .<sup>17</sup> Unless otherwise noted, we have performed calculations varying  $t'/t$ ,  $J/t$ ,  $h/t$ , and  $L$ ; for details of the DMRG calculations, see Ref. 18. In the interest of numerical stability, most runs were done at  $n_c = 1$ , but we have checked for selected  $J/t$  and  $t'/t$  and our conclusions remain robust also for  $n_c \neq 1$ .

The key quantity in our analysis is the impurity magnetization,  $M = \sum_i \langle S_i^z \rangle / L$ , as a function of applied impurity field  $h$  and system size  $L$ . Sample data for  $M/h$  are shown in Fig. 2. In all cases,  $M \propto h$  as  $h \rightarrow 0$ , which allows us to define the local impurity susceptibility  $\chi = M/h|_{h \rightarrow 0}$ . This quantity is seen to strongly depend on system size for small  $J$ . Indeed, for the standard case of an immobile impurity, the finite-size behavior of the susceptibility distinguishes 1CK and 2CK Kondo effects:  $\chi$  approaches a constant in the 1CK case,  $\chi \propto 1/T_K$ , whereas it diverges logarithmically with system size in the 2CK case,  $\chi \propto (1/T_K) \ln(T_K L)$ . The same qualitative behavior can be expected for mobile Kondo polarons—this is well borne out by our numerics: The data for  $\chi$  in Fig. 3 clearly show log-divergent  $\chi(1/L)$  for large  $t'$  and constant  $\chi(1/L)$  for small  $t'$ .

The distinct behavior at small and large  $J$  is further illustrated in the inset of Fig. 2, where the data points at fixed  $L$ ,  $J/t$ ,  $t'/t$ , and high fields,  $h/t > 2$ , are fitted to the 1CK strong-coupling expression<sup>17</sup>

$$M(h) = \frac{\chi_0 h}{\sqrt{1 + 4(\chi_0 h)^2}}, \quad (2)$$

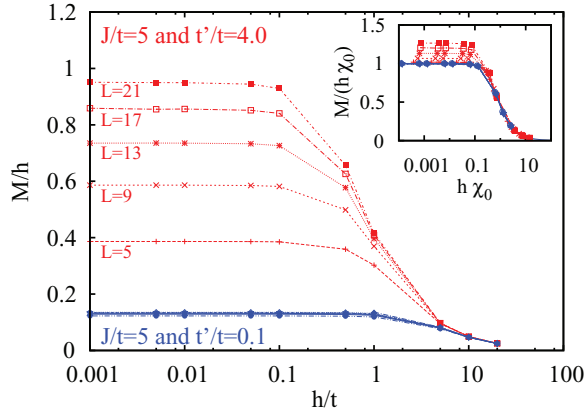


FIG. 2. (Color online) DMRG results for the impurity magnetization, plotted as  $M/h$ , as a function of  $h/t$  for  $L = 5, 9, 13, 17, 21$ . Data are shown for  $J/t = 5$ ,  $t'/t = 0.1$  (blue) and  $t'/t = 4$  (red), corresponding to the 1CK and 2CK phases, respectively. The inset shows the same data as  $M/(\chi_0 h)$  vs  $\chi_0 h$ , where  $\chi_0$  has been obtained from a fit at large fields to Eq. (2) (for details see text). Lines are guides to the eye.

and then plotted as  $M/(\chi_0 h)$  vs  $\chi_0 h$ . The large- $J$  data follow Eq. (2), again indicative of 1CK, whereas the small- $J$  data systematically deviate at small  $h$ , with a deviation increasing with increasing  $L$ .

To make the finite-size analysis of the susceptibility quantitative, we fit our DMRG data for  $\chi(L)$  utilizing the following crossover formulas:<sup>18,19</sup>

$$\chi_{1\text{CK}} = \frac{2\pi^2\Gamma + \Delta_L}{2(\pi^2\Gamma + \Delta_L)^2} \quad (3)$$

and

$$\chi_{2\text{CK}} = \frac{1}{2(\Delta_L + 4\pi^2\Gamma)} \ln \left[ 1 + \frac{4\Gamma\Delta_L + (4\pi\Gamma)^2}{\Delta_L^2} \right]. \quad (4)$$

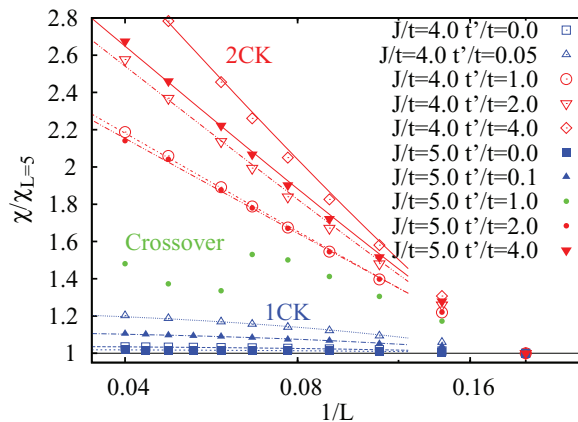


FIG. 3. (Color online) DMRG results for the local susceptibility  $\chi$  (divided by its value at length  $L = 5$ ) as a function of inverse system size  $1/L$  for parameter sets with  $J/t = 4$  and  $5$  and various  $t'/t$ . While the data at small  $t'$  show a clear saturation as  $L \rightarrow \infty$ , indicative of 1CK (blue),  $\chi$  at larger  $t'$  increases logarithmically, consistent with 2CK (red). The lines represent fits to Eqs. (3) and (4) (for details see text). One data set in the crossover region is also shown (green).

Here,  $\Gamma$  is an energy scale proportional to the (polaron) Kondo temperature, and  $\Delta_L = b/L$  parametrizes finite-size effects on the level spectrum. The formulas have been adopted from a finite-size bosonization analysis of the Kondo problem of an immobile impurity,<sup>19</sup> in this case  $\Delta_L$  represents the bath level spacing, with  $b = 4\pi t$  in the  $L \rightarrow \infty$  limit. Here we assume that Eqs. (3) and (4) provide reasonable descriptions of the data in the mobile-impurity case and for small  $L$  as well, but we treat  $b$  as a second fit parameter,  $b = b(t'/t, J/t)$ , in addition to  $\Gamma$ .

Fitting  $\chi(L)$  for all parameter sets (characterized by fixed values of  $J/t$ ,  $t'/t$ ,  $n_c = 1$ ) to both Eqs. (3) and (4) we observe the following: (i) Some data sets can be fitted well by only one of the two forms, allowing us to immediately discriminate between 1CK and 2CK behavior—this mainly applies if the data cover a range of  $\Delta_L/\Gamma = 0.1 \dots 1$ . (ii) Other data sets can be fitted by both forms, but often at the expense of extreme values of the fitting parameters. In particular,  $b/t \ll 1$  occurs when attempting to fit large- $J$  data with the 2CK form Eq. (4). The evolution of the fitting parameters with  $J$  and  $t'$  is nonmonotonic, which allows us to distinguish two regimes which clearly show 1CK and 2CK behavior, respectively.<sup>18</sup> (iii) At intermediate values of  $J$ , we observe data sets which are not well fitted with either of the two forms. Given that a putative QPT between 1CK and 2CK phases will be smeared for finite  $L$ , such behavior is consistent with the existence of a quantum critical transition regime. This interpretation is supported by our observation of significantly impaired convergence in this regime, which can be ascribed to long-range entanglement which cannot be well captured by the matrix product states underlying DMRG.

The existence of two distinct screening regimes, together with the quality of the fits, is demonstrated in Fig. 4, which shows a universality of  $\chi(L)$  when plotted as  $\chi\Gamma$  vs  $\Delta_L/\Gamma$ . Here, we have shown those data sets which could be uniquely

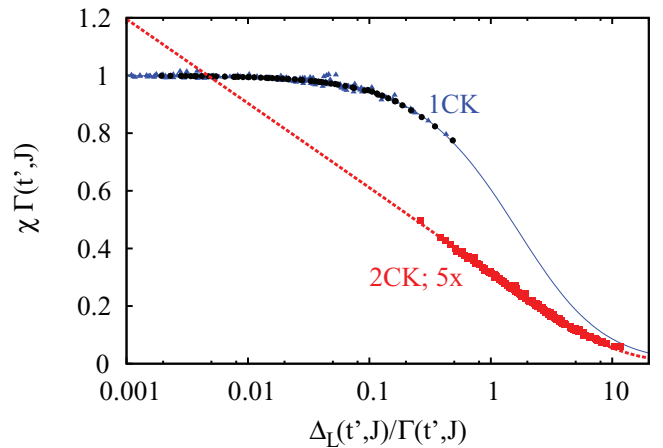


FIG. 4. (Color online) Scaling collapse of the DMRG results for the impurity susceptibility  $\chi(L; J/t, t'/t)$  in the 1CK and 2CK phases. In each of the phases,  $\chi\Gamma$  follows a universal behavior as a function of the finite-size parameter  $\Delta_L/\Gamma$  where  $\Delta_L = b/L$ , and  $\Gamma$  and  $b$  are fit parameters for each pair of  $J/t$  and  $t'/t$ . The symbols represent *all* data sets in Fig. 1, which could be uniquely associated with either 1CK (blue) or 2CK (red) behavior; the black symbols corresponds to  $t' = 0$ . The lines represent the scaling curves according to Eqs. (3) and (4); the data deviate from these at small  $L$ .

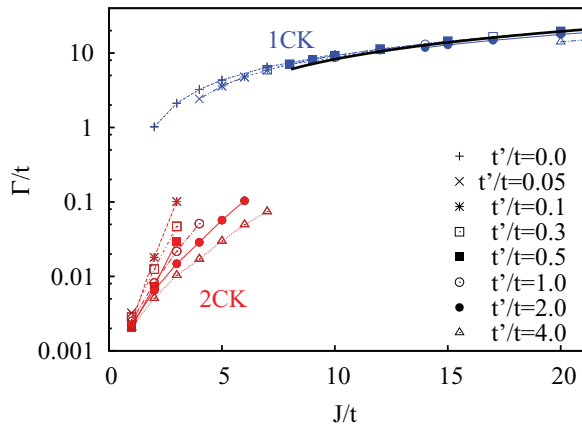


FIG. 5. (Color online) Kondo energy scale  $\Gamma$ , as extracted from the fits of  $\chi$  to Eqs. (3) and (4), as a function of  $J/t$  for different values of  $t'/t$  for the 1CK (2CK) regimes, shown in blue (red). The black line corresponds to  $\Gamma = J$ , indicating the strong-coupling behavior. Data points with  $\Gamma < 10^{-2}t$  are subject to severe finite-size effects as  $\xi_K \gg L$  here.

assigned to either the 1CK or the 2CK phase; deviations from universality occur for the data sets in the crossover region (for details see Ref. 18).

The fit parameter  $\Gamma$ , reflecting the polaron Kondo temperature  $T_K$ , is plotted in Fig. 5. First, we observe that 1CK behavior is seen for  $\Gamma > \min(t, t')$  as anticipated, whereas 2CK behavior is seen otherwise. Second,  $\Gamma$  becomes exponentially small for small  $J$  and is proportional to  $J$  for large  $J$ , as typical for the Kondo effect. Third,  $\Gamma$  is found to decrease with increasing  $t'$  in the 2CK regime. This can be rationalized by the fact that the motion of the Kondo polaron requires a spatial adjustment of the screening cloud which tends to suppress screening. In contrast,  $\Gamma$  is weakly dependent on  $t'$  in the 1CK regime, because here  $\Gamma > t'$ , i.e., the polaron moves sufficiently slowly for the screening cloud to adjust.

*Conclusions.* We have established that a spinful particle moving in a 1D Fermi gas displays a novel QPT between two phases with 1CK and 2CK screening of the particle's spin. While earlier perturbative arguments in favor of 2CK behavior apply to small Kondo coupling  $J$  only,  $T_K \ll \min(t', t)$ , our numerical results give evidence both for 1CK behavior at larger  $J$  and for a transition to 2CK upon decreasing  $J$ . We also find robust universal behavior in each phase which we fit using previous expressions from the static-impurity case. Finding the universal field theory for this QPT is an interesting open issue.

The model in Eq. (1) can in principle be realized using two species of atoms (with two hyperfine states each) in an optical lattice.<sup>20</sup> Due to the trapping potential, left and right movers will be coupled, such that the transition between 2CK and 1CK turns into a crossover. A suitable distinction between the two regimes is given by the low-temperature mobility, which follows  $T^{-2}$  ( $T^{-4}$ ) in the 2CK (1CK) case.<sup>3</sup> Alternatively, dilute spinful holes in doped semiconductor nanowires<sup>21</sup> can realize the model Eq. (1). Here, the change from local non-Fermi-liquid to Fermi-liquid behavior may be detected using the magnetic response in a Zeeman field, which is singular (regular) in the 2CK (1CK) case.<sup>7,19,22</sup>

Future work could possibly investigate the nonequilibrium dynamics near the Kondo-polaron QPT as well as the influence of bath interactions, i.e., the physics of Kondo polarons in a Luttinger liquid.

We thank B. Alascio, P. Cornaglia, A. Feiguin, E. Fradkin, T. Giamarchi, and C. Vojta for discussions. This research was supported by the DFG (FG 960), the German-Israeli Foundation, and the Early Career Research Program of US DOE. M.V. also acknowledges support by the Heinrich-Hertz-Stiftung NRW and the hospitality of the Centro Atómico Bariloche, where part of this work was performed.

<sup>1</sup>A. Rosch, *Adv. Phys.* **48**, 295 (1999).

<sup>2</sup>S. Palzer, C. Zipkes, C. Sias, and M. Köhl, *Phys. Rev. Lett.* **103**, 150601 (2009).

<sup>3</sup>A. Lamacraft, *Phys. Rev. Lett.* **101**, 225301 (2008).

<sup>4</sup>P. Nozières and A. Blandin, *J. Phys. (Paris)* **41**, 193 (1980).

<sup>5</sup>N. Andrei and C. Destri, *Phys. Rev. Lett.* **52**, 364 (1984); A. M. Tsvelik, *J. Phys. C* **18**, 159 (1985).

<sup>6</sup>I. Affleck and A. W. W. Ludwig, *Phys. Rev. Lett.* **67**, 161 (1991).

<sup>7</sup>D. L. Cox and A. Zawadowski, *Adv. Phys.* **47**, 599 (1998).

<sup>8</sup>R. M. Potok, I. G. Rau, H. Shtrikman, Y. Oreg, and D. Goldhaber-Gordon, *Nature (London)* **446**, 167 (2007).

<sup>9</sup>S. Sachdev, *Quantum Phase Transitions*, 2nd ed. (Cambridge University Press, Cambridge, UK, 2010).

<sup>10</sup>M. Vojta, *Philos. Mag.* **86**, 1807 (2006).

<sup>11</sup>C.-H. Chung and S. Silotri, *arXiv:1201.5610*.

<sup>12</sup>M. Fabrizio and A. O. Gogolin, *Phys. Rev. B* **51**, 17827 (1995).

<sup>13</sup>T. Fukuhara, A. Kantian, M. Endres, M. Cheneau, P. Schauß, S. Hild, D. Bellem, U. Schollwöck, T. Giamarchi, C. Gross,

I. Bloch, and S. Kuhr, *Nat. Phys.* **9**, 235 (2013); Y. Kato, K. A. Al-Hassanieh, A. E. Feiguin, E. Timmermans, and C. D. Batista, *Europhys. Lett.* **98**, 46003 (2012).

<sup>14</sup>C. D. Batista, J. Eroles, M. Avignon, and B. Alascio, *Phys. Rev. B* **58**, R14689 (1998); **62**, 15047 (2000).

<sup>15</sup>S. R. White, *Phys. Rev. Lett.* **69**, 2863 (1992); *Phys. Rev. B* **48**, 10345 (1993).

<sup>16</sup>K. Hallberg, *Adv. Phys.* **55**, 477 (2006); U. Schollwöck, *Rev. Mod. Phys.* **77**, 259 (2005).

<sup>17</sup>X. Wang, *Mod. Phys. Lett. B* **12**, 667 (1998).

<sup>18</sup>See Supplemental Material at <http://link.aps.org/supplemental/10.1103/PhysRevB.88.140407> for details of the DMRG calculation, a derivation of the fitting formulas, and additional numerical results and their finite-size fitting.

<sup>19</sup>G. Zarand and J. von Delft, *Phys. Rev. B* **61**, 6918 (2000).

<sup>20</sup>L. M. Duan, *Europhys. Lett.* **67**, 721 (2004); M. Foss-Feig, M. Hermele, and A. M. Rey, *Phys. Rev. A* **81**, 051603(R) (2010).

<sup>21</sup>J. Calleja, *Solid State Commun.* **79**, 911 (1991).

<sup>22</sup>V. J. Emery and S. Kivelson, *Phys. Rev. B* **46**, 10812 (1992).